

DOI: <http://dx.doi.org/10.1590/1807-1929/agriambi.v27n5p317-326>

## Abiotic factors and photosynthetically active photon density affect the physiological mechanisms of jaboticaba<sup>1</sup>

Fatores abióticos e densidade de fótons fotossinteticamente ativos afetam os mecanismos fisiológicos de jaboticaba

Ester dos S. Coêlho<sup>2</sup>, João E. da S. Ribeiro<sup>2\*</sup>, Elania F. da Silva<sup>2</sup>, Toshik I. da Silva<sup>3</sup>,  
Pablo H. de A. Oliveira<sup>2</sup>, Thiago J. Dias<sup>4</sup>, Aurélio P. Barros Júnior<sup>2</sup>,  
Daniel V. Silva<sup>2</sup> & Ronald M. Rodriguez<sup>5</sup>

<sup>1</sup> Research developed at Universidade Federal Rural do Semi-Árido, Mossoró, RN, Brazil

<sup>2</sup> Universidade Federal Rural do Semi-Árido, Mossoró, RN, Brazil

<sup>3</sup> Universidade Federal de Viçosa, Viçosa, MG, Brazil

<sup>4</sup> Universidade Federal da Paraíba, Areia, PB, Brazil

<sup>5</sup> University of Geneva/Laboratory of Fluoromatics, Geneva, Switzerland

### HIGHLIGHTS:

*Higher air temperature and photosynthetic photon flux density provide greater net CO<sub>2</sub> assimilation in Plinia peruviana plants. The increase in photosynthetically active photon density up to 1000 μmol m<sup>-2</sup> s<sup>-1</sup> positively influenced physiology of species. The gas exchange and chlorophyll a fluorescence of P. peruviana were altered due to environmental conditions.*

**ABSTRACT:** In fruit species, the amount of solar energy absorbed can influence fruit quality; hence, ensuring optimal light distribution management in the canopy of plants is essential. Therefore, the objectives of this study were (i) to analyze the variations in gas exchange through the day and (ii) identify the photosynthetically active photon flux density (PPFD) that promotes higher chlorophyll fluorescence and electron transport rate in jaboticaba seedlings. The experimental design was completely randomized, with treatments consisting of 18 photosynthetic photon flux densities and three evaluations throughout the day. Six replicates were used, with two plants per plot. Gas exchange and chlorophyll a fluorescence in *P. peruviana* were altered due to fluctuating photosynthetic photon flux density (0; 25; 50; 75; 100; 125; 150; 175; 200; 400; 600; 800; 1,000; 1,200; 1,400; 1,600; 1,800; and 2,000 μmol m<sup>-2</sup> s<sup>-1</sup>) and environmental conditions throughout the day (8:00 a.m., 12:00 and 4:00 p.m.). The higher PPFD (1,384.6 μmol m<sup>-2</sup> s<sup>-1</sup>) and air temperature (39.74 °C) at noon (12:00 p.m.) favored gas exchange in this species. An increase in PPFD of up to 1,000 μmol m<sup>-2</sup> s<sup>-1</sup> positively influenced the gas exchange and chlorophyll a fluorescence of *P. peruviana*.

**Key words:** *Plinia peruviana*, photosynthesis, Myrtaceae

**RESUMO:** Em espécies fruteiras, é essencial considerar o gerenciamento da distribuição da luz nas copas das plantas, pois a quantidade de energia solar absorvida pode influenciar na qualidade dos frutos. Diante disso, os objetivos deste estudo foram: (i) analisar as variações das trocas gasosas ao longo do dia; (ii) identificar a densidade de fluxo de fótons fotossinteticamente ativos (PPFD) que promove maior fluorescência da clorofila e maior taxa de transporte de elétrons em mudas de jaboticaba. O delineamento experimental foi inteiramente casualizado, sendo os tratamentos compostos por 18 densidades de fluxo de fótons fotossinteticamente ativos (0; 25; 50; 75; 100; 125; 150; 175; 200; 400; 600; 800; 1.000; 1.200; 1.400; 1.600; 1.800 e 2.000 μmol m<sup>-2</sup> s<sup>-1</sup>) e três horários de avaliação ao longo do dia (08:00, 12:00 e 16:00 h). Foram utilizadas seis repetições, considerando duas plantas por parcela útil. Trocas gasosas e fluorescência da clorofila a de *P. peruviana* foram alterados em virtude da PPFD e das condições ambientais ao longo do dia. A alta PPFD (1.384,6 μmol m<sup>-2</sup> s<sup>-1</sup>) e temperatura do ar (39,74 °C) no horário de 12 horas favoreceu as trocas gasosas dessa espécie. O aumento da PPFD até 1.000 μmol m<sup>-2</sup> s<sup>-1</sup> influenciou positivamente as trocas gasosas e fluorescência da clorofila a de *P. peruviana*.

**Palavras-chave:** *Plinia peruviana*, fotossíntese, Myrtaceae

• Ref. 267479 – Received 01 Sept, 2022

\* Corresponding author - E-mail: [j.everthon@hotmail.com](mailto:j.everthon@hotmail.com)

• Accepted 26 Nov, 2022 • Published 15 Dec, 2022

Editors: Geovani Soares de Lima & Walter Esfrain Pereira

This is an open-access article distributed under the Creative Commons Attribution 4.0 International License.



## INTRODUCTION

Abiotic stressors induce varied physiological responses in plants (Zhang et al., 2021). Among these factors, temperature, water, nutritional availability, luminosity, and relative humidity modulate the metabolic and morphophysiological responses of plants (Saijo & Loo, 2020). In fruit species such as jaboticaba [*Plinia peruviana* (Poir.) Govaerts], ensuring light distribution management in the canopy is essential because the amount of solar energy absorbed can influence fruit quality. Jaboticaba can be found in South American countries such as Mexico, Bolivia, Argentina, Paraguay, and Brazil, with Brazil being its largest producer in the world (Baptistella & Coelho, 2019). Among the Brazilian states, Goiás is the largest producer; Paraíba produces 203 tons and is the fourth largest producer in the country (IBGE, 2017).

Reduced or excessive light intensity can cause changes in growth, development, productivity, and dry matter content of plants. However, plants adjust to these conditions through various mechanisms because the physiological variables involved in photosynthesis and leaf characteristics are adapted according to light availability. The photosynthetic photon flux density (PPFD) corresponded to the light intensity available during photosynthesis (Poorter et al., 2019). Therefore, the PPFD demonstrates the relationship between the incident irradiance on the leaf surface and the photosynthetic rate reflected in its response curve. This relationship is necessary to understand the current state of leaf acclimatization and plant productivity in specific environments.

We hypothesized that the gas exchange and chlorophyll fluorescence of jaboticaba (*P. peruviana*) present variations owing to the light intensity provided throughout the day. The objectives of this study were: (i) to analyze the variations in gas exchange throughout the day and (ii) to identify the PPFD

that promotes higher chlorophyll fluorescence and electron transport rate in *Plinia peruviana* seedlings.

## MATERIAL AND METHODS

This study was conducted in a protected environment located in the forest nursery of the Department of Plant Sciences and Environmental Sciences, Universidade Federal da Paraíba, Areia municipality, Paraíba, Northeastern Brazil (6° 57' 59" S and 35° 42' 57" W - 506 m of altitude). This region is a part of the mesoregion of Agreste Paraibano and microrregião of Brejo Paraibano, with an average temperature of approximately 22 °C and an average precipitation of approximately 1,400 mm per year (Ribeiro et al., 2018). The climate is classified as tropical with dry and hot summers and winter rains (Alvares et al., 2013).

This study was conducted between January 2017 and January 2021. During the study period, the environmental climatic data were measured daily; the average recorded values within the protected environment were 24.1 °C for atmospheric temperature and 55.2% for relative humidity (Figure 1). Climatic data were collected using a digital thermo-hygrometer (Minipa, model MT-241A).

For seedling production, mature fruits were collected from the mother trees located in the municipality of Areia. After collection, the seeds were extracted from the fruits, cleaned, and the endocarp was completely removed from the seed tegument. The seeds were sown in plastic pots with a capacity of 25 dm<sup>3</sup> filled with a soil and commercial substrate (3:1, v/v). Oxisol soil was used (United States, 2014), which is classified as a Latossolo Vermelho-Amarelo in the Brazilian Soil Classification System (EMBRAPA, 2018). The physical-chemical attributes of substrate were: pH (H<sub>2</sub>O): 6.12; P: 118.7 mg dm<sup>-3</sup>; K<sup>+</sup>: 217.2 mg dm<sup>-3</sup>; Na<sup>+</sup>: 0.43 cmol<sub>c</sub> dm<sup>-3</sup>; H<sup>+</sup> + Al<sup>3+</sup>:

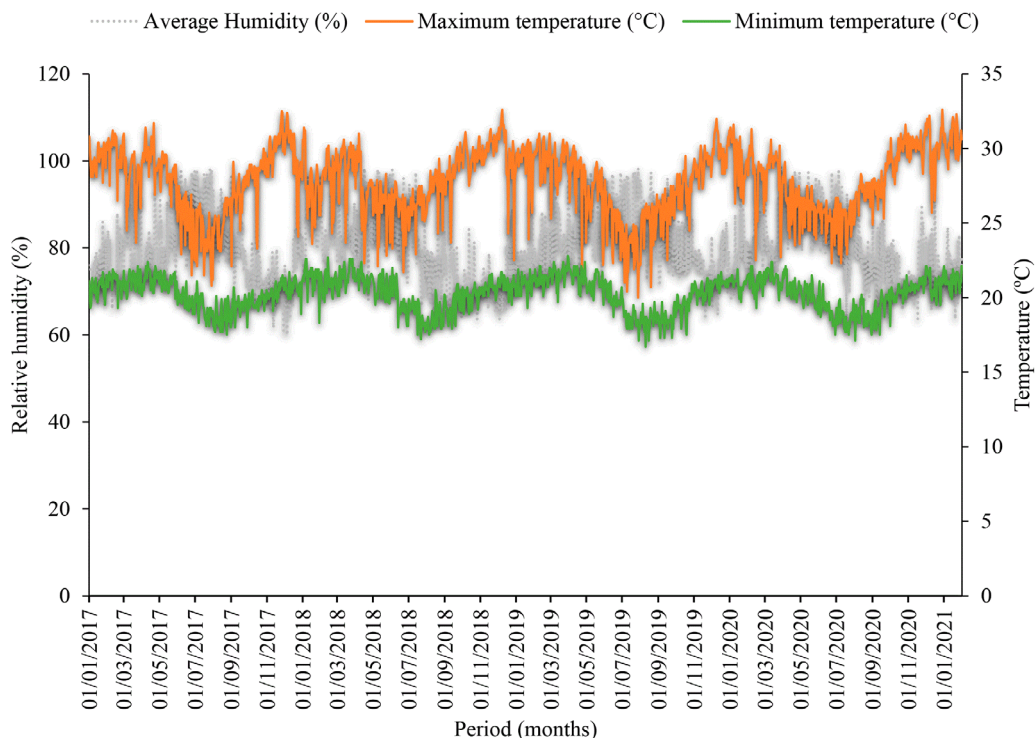


**Figure 1.** Air temperature and relative air humidity during the experimental period

4.62 cmol<sub>c</sub> dm<sup>-3</sup>; Al<sup>3+</sup>: 0.00 cmol<sub>c</sub> dm<sup>-3</sup>; Ca<sup>2+</sup>: 3.5 cmol<sub>c</sub> dm<sup>-3</sup>; Mg<sup>2+</sup>: 3.1 cmol<sub>c</sub> dm<sup>-3</sup>; sum of bases: 7.58 cmol<sub>c</sub> dm<sup>-3</sup>; cation exchange capacity: 12.2 cmol<sub>c</sub> dm<sup>-3</sup>; base saturation: 62.1%; organic matter: 29.86 g kg<sup>-1</sup>; sand: 650 g kg<sup>-1</sup>; silt: 165 g kg<sup>-1</sup>; and clay: 185 g kg<sup>-1</sup>. The physicochemical attributes of the soil were analyzed according to the methodology proposed by EMBRAPA (2017).

Five seeds per pot were planted, and thinning was performed when the seedlings were approximately 10 cm tall, retaining one individual per pot. Irrigation was performed daily, and the gravimetric method was used to maintain a field capacity of approximately 80%.

The experimental design was completely randomized, and 18 photosynthetically active photon flux densities (0; 25; 50; 75; 100; 125; 150; 175; 200; 400; 600; 800; 1,000; 1,200; 1,400; 1,600; 1,800; and 2,000 μmol m<sup>-2</sup> s<sup>-1</sup>) were tested thrice through the day (8:00 a.m., 12:00 and 4:00 p.m.). Six replicates were used, with two plants per useful plot; therefore, 12 individuals were evaluated at each evaluation time point. The evaluations were performed in plants with an average height of 1.45 ± 0.27 m four years after planting; with daily readings were taken daily.

The internal (InT) and external temperatures (ExT) and relative internal (InRH) and external air humidity (ExRH) of the protected environment were measured during the physiological evaluations using a digital thermo-hygrometer (Minipa, model MT-241A). PPFd was measured using a natural light sensor coupled to a portable infrared carbon dioxide analyzer (IRGA) (LI-COR, model LI-6400XT).

Gas exchange analyses were performed using Infra-red gas analyzer (IRGA) (LI-COR, model LI-6400XT), and the net CO<sub>2</sub> assimilation rate (A) (μmol CO<sub>2</sub> m<sup>-2</sup> s<sup>-1</sup>), stomatal conductance (g<sub>s</sub>) (mol m<sup>-2</sup> s<sup>-1</sup>), transpiration rate (E) (mmol H<sub>2</sub>O m<sup>-2</sup> s<sup>-1</sup>), internal CO<sub>2</sub> concentration (C<sub>i</sub>) (μmol CO<sub>2</sub> mol<sup>-1</sup>), and instantaneous carboxylation efficiency [iCE (A/C<sub>i</sub>)] [(μmol CO<sub>2</sub> m<sup>-2</sup> s<sup>-1</sup>) (μmol CO<sub>2</sub> mol<sup>-1</sup>)<sup>-1</sup>] were analyzed. Chlorophyll fluorescence analysis was performed using a fluorometer (LI-COR, model LI-6400-40 LCF) coupled with the IRGA. The initial fluorescence (F<sub>0</sub>'), maximum fluorescence (F<sub>m</sub>'), variable fluorescence (F<sub>v</sub>'), quantum efficiency of PSII (F<sub>v</sub>'/F<sub>m</sub>'), ratio between variable and initial fluorescence (F<sub>v</sub>'/F<sub>0</sub>'), and electron transport rate (ETR) were determined in leaves subjected to a saturating flash of actinic irradiation and a pulse of light in the distant red region.

The measurements were performed on healthy leaves that were free of damage, pests, or diseases, and wholly expanded in the median third of the plants. Four leaves per plant were analyzed. The following measurement protocol was used in the IRGA chamber: relative humidity, 50–60%; 300 μmol s<sup>-1</sup> airflow; CO<sub>2</sub> concentration, 400 μmol mol<sup>-1</sup>; and area of artificial light sensor in the leaf chamber, 2 cm<sup>2</sup>.

The response curves of gas exchange and chlorophyll fluorescence to PPFd were obtained in increments from 200–2,000 μmol m<sup>-2</sup> s<sup>-1</sup> at intervals of 200 μmol m<sup>-2</sup> s<sup>-1</sup>. Below 200 μmol m<sup>-2</sup> s<sup>-1</sup> up to 0, the PPFd was varied at 25 μmol m<sup>-2</sup> s<sup>-1</sup> intervals to obtain the apparent quantum efficiency (Φ [μmol CO<sub>2</sub> μmol<sup>-1</sup> photons]). The apparent quantum efficiency was estimated by adjusting a linear equation in the range in which the variation of A as a function of the PPFd was linear; A =

a + Φ.Q, where a and Φ are adjustment coefficients and the PPFd is represented by Q. The luminous compensation point was obtained as Γ (μmol m<sup>-2</sup> s<sup>-1</sup>) at the point of intersection of the line with the x-axis. The response curve of A as a function of the PPFd was adjusted to a rectangular hyperbolic function:

$$A = \frac{A_{\max} \times Q}{a + Q} \quad (1)$$

where:

- A - net CO<sub>2</sub> assimilation rate;
- Q - photosynthetically active photon flux density;
- A<sub>max</sub> - maximum rate of photosynthesis; and,
- a - coefficient of equation adjustment.

The data were subjected to nonlinear regression analysis, and the rectangular hyperbolic function was adjusted. Pearson correlation and principal component analysis (PCA) were performed to verify the relationship between environmental (PPFD, InT, ExT, InRH, and ExRH) and physiological (A, g<sub>s</sub>, E, C<sub>i</sub>, F<sub>0</sub>', F<sub>m</sub>', F<sub>v</sub>', F<sub>v</sub>'/F<sub>m</sub>', F<sub>v</sub>'/F<sub>0</sub>' and ETR) variables. The analyses were performed using R<sup>v</sup> 4.1.1 (R Core Team, 2022).

## RESULTS AND DISCUSSION

The environmental components varied at the different evaluation times (Figure 2). The highest PPFd was observed at 12:00 p.m. (1384.60 μmol m<sup>-2</sup> s<sup>-1</sup>) and the lowest at 4:00 p.m. (147.00 μmol m<sup>-2</sup> s<sup>-1</sup>) (Figure 2). The same trend was observed for the internal and external environmental temperatures, which were recorded at 12:00 p.m. [39.74 °C (InT), and 39.68 °C (ExT)] (Figure 2). However, the internal and external relative humidity was lower when the temperature and PPFd were higher, and the highest values were recorded [55.8% (InRH) and 58% (ExRH)] and 4:00 p.m. [40.10% (InRH) and 52.72% (ExRH)] (Figure 2).

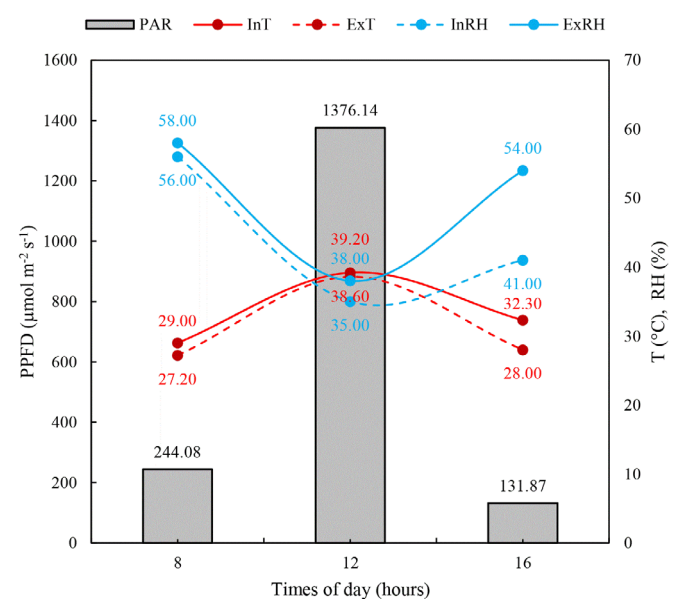
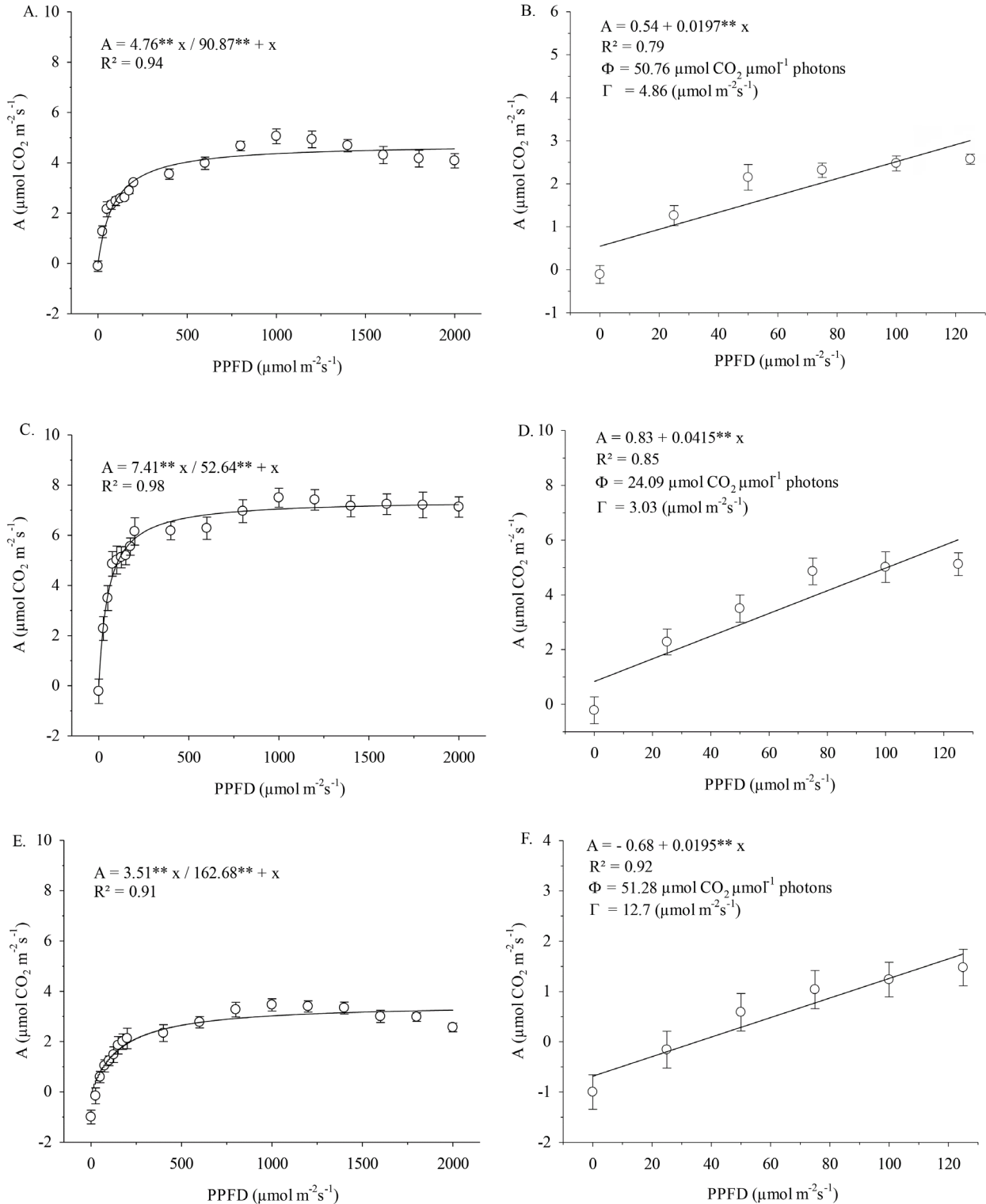


**Figure 2.** Photosynthetic photon flux density (PPFD), internal (InT) and external (ExT) air temperatures, and internal (InRH) and external (ExRH) relative air humidity of the environment (greenhouse) as a function of hours of day

In the present study, we observed that as the temperature and PPFD increased, relative humidity of the environment decreased. Thus, the combined action of the environmental factors could directly influence physiological processes (Cordeiro et al., 2020; Sharma et al., 2020). In addition, these abiotic components may induce changes in the composition of plant tissues, particularly in the leaf cuticle. A high temperature during warmer times of the day, which associated

with a reduction in relative humidity, could reduce water permeability through a change in cuticle components such as waxes. Regarding physiological mechanisms, the oscillation of environmental factors can cause limitations in photosynthesis through stomatal closure or reduced ribulose-1,5-biphosphate carboxylase oxygenase enzyme activity (Liu et al., 2014).

The net CO<sub>2</sub> assimilation rate (A) was observed as PPFD increased (Figure 3). At all evaluation time points, the highest



\*\* - Significant at  $p \leq 0.01$  by F test; \* - Significant at  $p \leq 0.05$  by F test; ns - Not significant by F test

**Figure 3.** Net CO<sub>2</sub> assimilation rate (A), apparent quantum efficiency ( $\Phi$ ), and the light compensation point ( $\Gamma$ ) in *Plinia peruviana* plants as a function of photosynthetic photon flux density (PPFD) at different times of day [(A, B) 8:00 a.m.; (C, D) 12:00 p.m.; (E, F) 4:00 p.m.]. Bars represent standard deviation

values were recorded at a PPFD of  $1000 \mu\text{mol m}^{-2} \text{s}^{-1}$  (Figure 3). Among the three evaluation time points, the highest A ( $7.039 \mu\text{mol CO}_2 \text{ m}^{-2} \text{s}^{-1}$ ) was observed at 12:00 p.m. (Figure 3C). However, despite the highest A being observed at a PPFD of  $1000 \mu\text{mol m}^{-2} \text{s}^{-1}$  at the other two time points also, a 32.60 and 53.86% reduction, respectively, was observed (Figures 3A and E).

The apparent quantum efficiencies ( $\Phi$ , coefficient of the linear region of the light response curve) recorded were 24.09 (12:00 p.m.), 50.76 (8:00 a.m.), and 51.28 (4:00 p.m.)  $\mu\text{mol CO}_2 \mu\text{mol}^{-1}$  photons (Figure 3B, D and F). According to this quotient, to fix one mole of  $\text{CO}_2$ , 24.09 (12:00 p.m.), 50.76 (8:00 p.m.), and 51.28 (4:00 p.m.)  $\mu\text{mol}$  photons are needed, indicating a difference in the efficiency of usage of ATP and NADPH during the Calvin cycle. The luminous compensation points ( $\Gamma$ ) were 4.86 at 8:00 a.m., 3.03 at 12:00 p.m., and  $12.7 \mu\text{mol m}^{-2} \text{s}^{-1}$  at 4:00 p.m., respectively (Figures 3B, D and F).

The results obtained indicate that high PPFD favored the net  $\text{CO}_2$  assimilation rate (A), which can be explained as an adaptation of plants to high light intensity to maximize photon absorption and the efficiency of the use of photosynthetic light. Thus, the effects of PPFD and high temperature at 12:00 p.m., which showed the highest net  $\text{CO}_2$  assimilation rate, were verified.

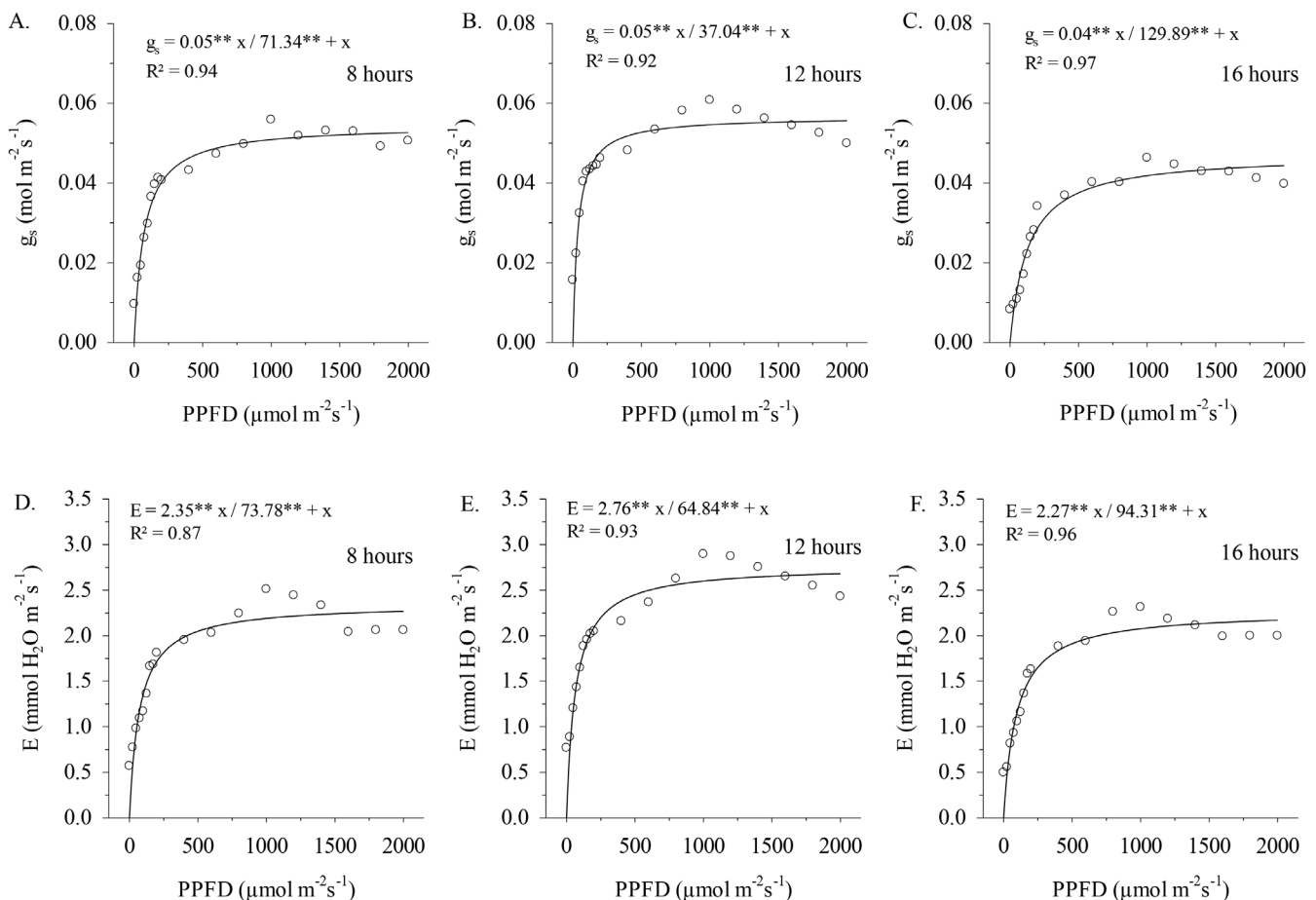
At all evaluation times, stomatal conductance ( $g_s$ ) increased until the PPFD reached  $1000 \mu\text{mol m}^{-2} \text{s}^{-1}$ , with the highest value ( $0.0482 \text{ mol m}^{-2} \text{s}^{-1}$ ) recorded at 12:00 p.m. (Figure 4B).

The lowest record at the PPFD of  $1000 \mu\text{mol m}^{-2} \text{s}^{-1}$  was at 4:00 p.m., which showed a 53.85% reduction (Figure 4C).

The decrease in A and  $g_s$  observed after reaching a PPFD of  $1000 \mu\text{mol m}^{-2} \text{s}^{-1}$  may be a response to light saturation at higher photon densities (Larsen et al., 2020). Responses to light intensity are known to vary according to the species and growth environment (Larsen et al., 2020). Stomatal conductance is regulated by the turbidity of the guard cells and the interception of light, which indicates that the high PPFD recorded at 12:00 favored the opening of the stomata (Ribeiro & Coêlho, 2021). At higher temperatures, plants increase the  $g_s$  to maintain leaf temperature, indicating a state of acclimatization (Fauset et al., 2019). Some studies have indicated that acclimatization of the net  $\text{CO}_2$  assimilation rate and stomatal conductance due to the increase in air temperature throughout the day can occur through changes in membrane fluidity, increased activity of RuBisCO activase, and the expression of proteins that condition thermal protection (Fauset et al., 2019).

The transpiration rate (E) showed results similar to stomatal conductance ( $g_s$ ), with the highest increases noticed until PPFD reached  $1000 \mu\text{mol m}^{-2} \text{s}^{-1}$ , and the highest record value was  $2.5919 \text{ mmol H}_2\text{O m}^{-2} \text{s}^{-1}$  at 12:00 p.m. (Figure 4E). A similar behavior was observed in the values recorded at 8:00 a.m. and 4:00 p.m. (Figures 4D and F).

The results obtained for transpiration (E) indicated an association between transpiration and stomatal conductance (Griebel et al., 2020). Most plant species close their stomata



\*\* - Significant at  $p \leq 0.01$  by F test; \* - Significant at  $p \leq 0.05$  by F test; ns - No significant by F test

**Figure 4.** Stomatal conductance ( $g_s$ ) [(A) 8:00 a.m.; (B) 12:00 p.m.; (C) 4:00 p.m.] and transpiration (E) [(D) 8:00 a.m.; (E) 12:00 p.m.; (F) 4:00 p.m.] in *P. peruviana* plants as a function of photosynthetic photon flux density (PPFD) at different times of the day

at warmer times of the day to prevent water loss. This closure reduces the photosynthetic rate and respiration. However, some isolated cases have been reported where the maintenance of transpiration and photosynthesis through stomatal regulation causes cooling of the leaves and allows acclimatization at higher temperatures (De Kauwe et al., 2019). In the present study, E and stomatal conductance values were higher at 12:00 p.m.

The  $C_i$  drastically decreases with the increase in PPFD, and the highest recorded values were 635.79 and 662.69  $\mu\text{mol CO}_2 \text{ mol}^{-1}$  at 8:00 a.m. and 4:00 p.m., respectively (Figures 5A and C). For this variable, the highest recorded values at all evaluation time points, were observed at the PPFD of 0  $\mu\text{mol m}^{-2} \text{ s}^{-1}$  (Figures 5A, B, and C).

$C_i$  is related to the supply and demand of  $\text{CO}_2$  for photosynthesis. This factor is associated with turgor and leaf temperature, irradiance interception, and vapor pressure deficit, which modulate stomatal regulation (Griebel et al., 2020; Ribeiro et al., 2022). In the present study, we detected that the highest stomatal conductance ( $g_s$ ) and net  $\text{CO}_2$  assimilation rate (A) values allowed for the reduction of intercellular carbon. The results confirmed the theory proposed by Fauset et al. (2019), that a reduction in stomatal conductance maintains a high  $C_i$ .

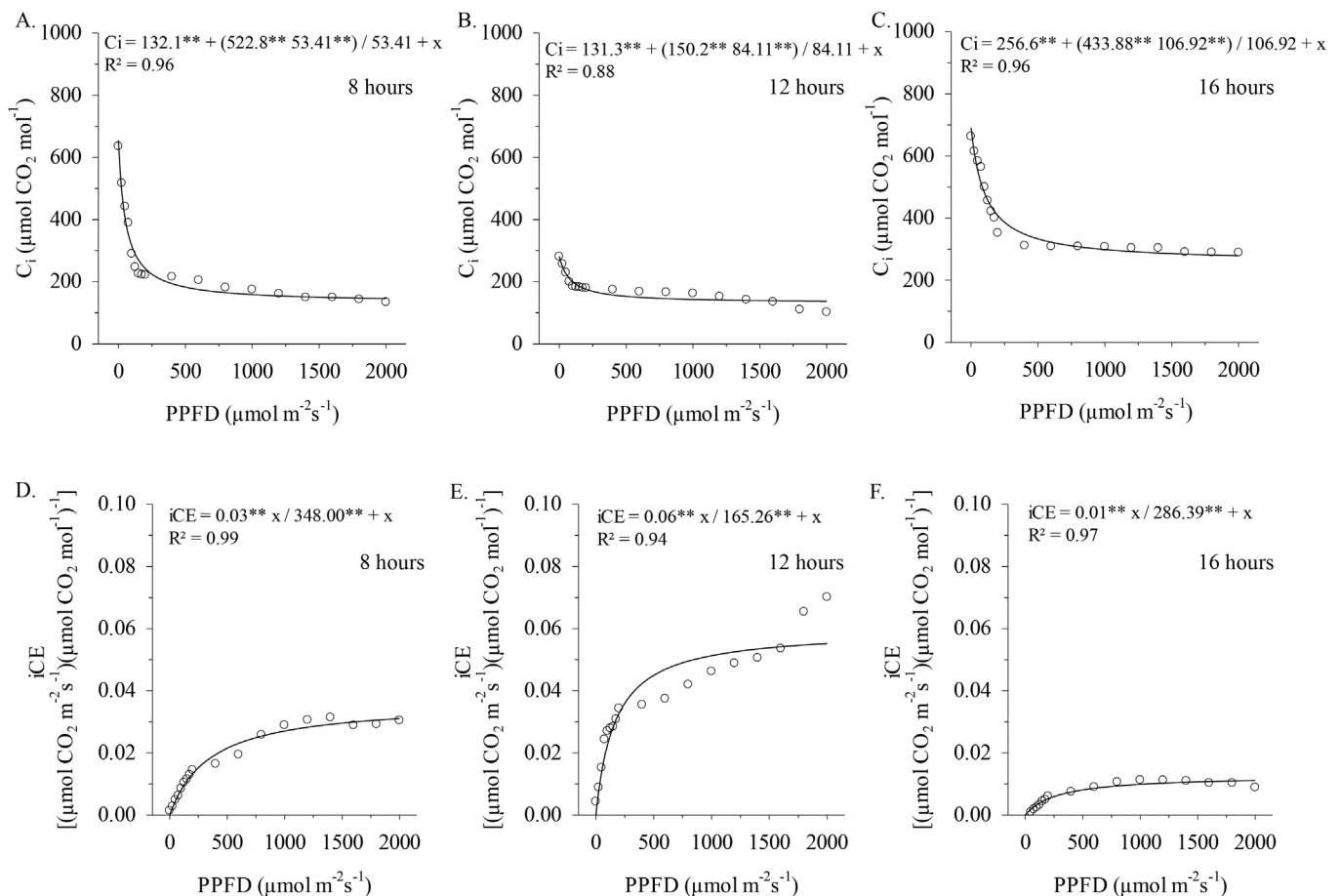
The instantaneous carboxylation efficiency (iCE) increased with increase in PPFD; the highest recorded value of 0.0701 [ $(\mu\text{mol CO}_2 \text{ m}^{-2} \text{ s}^{-1}) (\mu\text{mol CO}_2 \text{ mol}^{-1})^{-1}$ ] (Figure 5E)

corresponded to a PPFD of 2000  $\mu\text{mol m}^{-2} \text{ s}^{-1}$  at 12:00 p.m. The highest recorded values at 8:00 a.m. and 4:00 p.m., were 0.0313 and 0.0314 [ $(\mu\text{mol CO}_2 \text{ m}^{-2} \text{ s}^{-1}) (\mu\text{mol CO}_2 \text{ mol}^{-1})^{-1}$ ], respectively, and corresponded to a PPFD of 1400  $\mu\text{mol m}^{-2} \text{ s}^{-1}$  (Figures 5D and F).

The changes noticed in the environmental conditions during the different evaluation time points conditioned the acclimatization of *P. peruviana* plants. Thus, the effects of changes in photosynthesis and  $C_i$  reflect the instantaneous carboxylation efficiency. Higher carboxylation efficiency indicates a higher amount and activity of ribulose-1,5-biphosphate carboxylase oxygenase and more efficient use of carbon in leaf mesophiles (Barbosa et al., 2019).

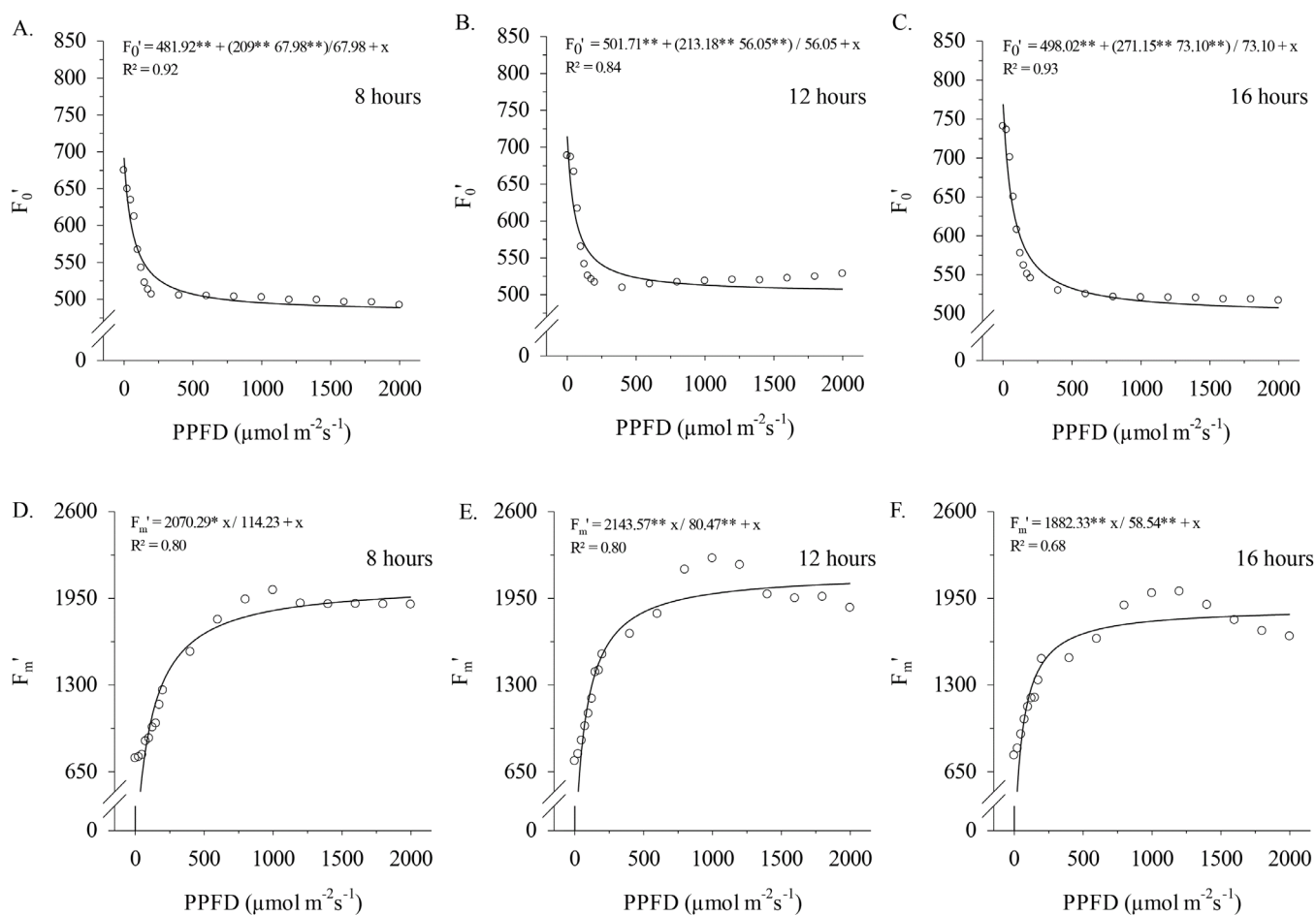
The initial fluorescence ( $F_0'$ ) showed similar trends at all times, with the highest values of 688.46 and 740.65 quantum electrons $^{-1}$  recorded at a PPFD density of 0  $\mu\text{mol m}^{-2} \text{ s}^{-1}$  at 12:00 p.m. and 4:00 p.m., respectively (Figures 6B and C). The values recorded for maximum fluorescence ( $F_m'$ ) increased as the PPFD increased. The highest recorded value was 2250.0 quantum electrons $^{-1}$  at the PPFD of 1000  $\mu\text{mol m}^{-2} \text{ s}^{-1}$  at 12:00 p.m. (Figure 6E). After the PPFD of 1000  $\mu\text{mol m}^{-2} \text{ s}^{-1}$  was attained, a 15.4, 16.5, and 26.0% reduction in fluorescence was noticed at the respective evaluation time points (Figures 6D, E and F).

The increase in the initial fluorescence ( $F_0'$ ) values may be associated with an established stress condition for plants,



\*\* - Significant at  $p \leq 0.01$  by F test; \* - Significant at  $p \leq 0.05$  by F test; ns - No significant by F test

**Figure 5.** Internal  $\text{CO}_2$  concentration ( $C_i$ ) [(A) 8:00 a.m.; (B) 12:00 p.m.; (C) 4:00 p.m.] and instantaneous carboxylation efficiency (iCE) [(D) 8:00 a.m.; (E) 12:00 p.m.; (F) 4:00 p.m.] in *P. peruviana* plants as a function of photosynthetic photon flux density (PPFD) at different times of the day



\*\* - Significant at  $p \leq 0.01$  by F test; \* - Significant at  $p \leq 0.05$  by F test; <sup>ns</sup> - No significant by F test

**Figure 6.** Initial  $F_0'$  [(A) 8:00 a.m.; (B) 12:00 p.m.; (C) 4:00 p.m.] and maximum fluorescence ( $F_m'$ ) [(D) 8:00 a.m.; (E) 12:00 p.m.; (F) 4:00 p.m.] in *P. peruviana* plants as a function of photosynthetic photon flux density (PPFD) at different times of the day

which was at the lowest PPFD in the present study. Therefore, the increase in  $F_0'$  indicates a change in the PSII reaction center or disruption in the transfer of absorbed light energy. Maximum fluorescence ( $F_m'$ ) occurs by transferring the energy required for the reduction of NADPH and ferredoxin, which promotes a good performance in the photochemical stage of photosynthesis and enables the formation of ATP for CO<sub>2</sub> assimilation. Under stress conditions, the reduction of  $F_m'$  indicates a decrease in quinone due to the inactivation of PSII and the influence on electron transport between photosystems (Miller et al., 2020).

The variable fluorescence ( $F_v'$ ) and quantum efficiency of PSII ( $F_v'/F_m'$ ) showed similar trends, with values showing an increase when PPFD increased and being constant when PPFD increased above of 1000  $\mu\text{mol m}^{-2} \text{s}^{-1}$  (Figure 7). The highest value for  $F_v'$  was 1731.4 quantum electrons<sup>-1</sup> and was recorded at 12:00 p.m. (Figure 7B). However, a reduction by 12.8 and 15.2% was noticed at the same PPFD of 1000  $\mu\text{mol m}^{-2} \text{s}^{-1}$  at 8:00 a.m. and 4:00 p.m., respectively (Figures 7A and C).

The results obtained for  $F_v'$  at the PPFD of 1000  $\mu\text{mol m}^{-2} \text{s}^{-1}$  may have provided greater stability for the electron transfer process in the photochemical step (Souza et al., 2019). These fluorescence parameters are important for predicting the proper functioning of photochemistry and non-photochemical de-excitation, which can occur when plants are exposed to adverse environmental conditions. The variations observed

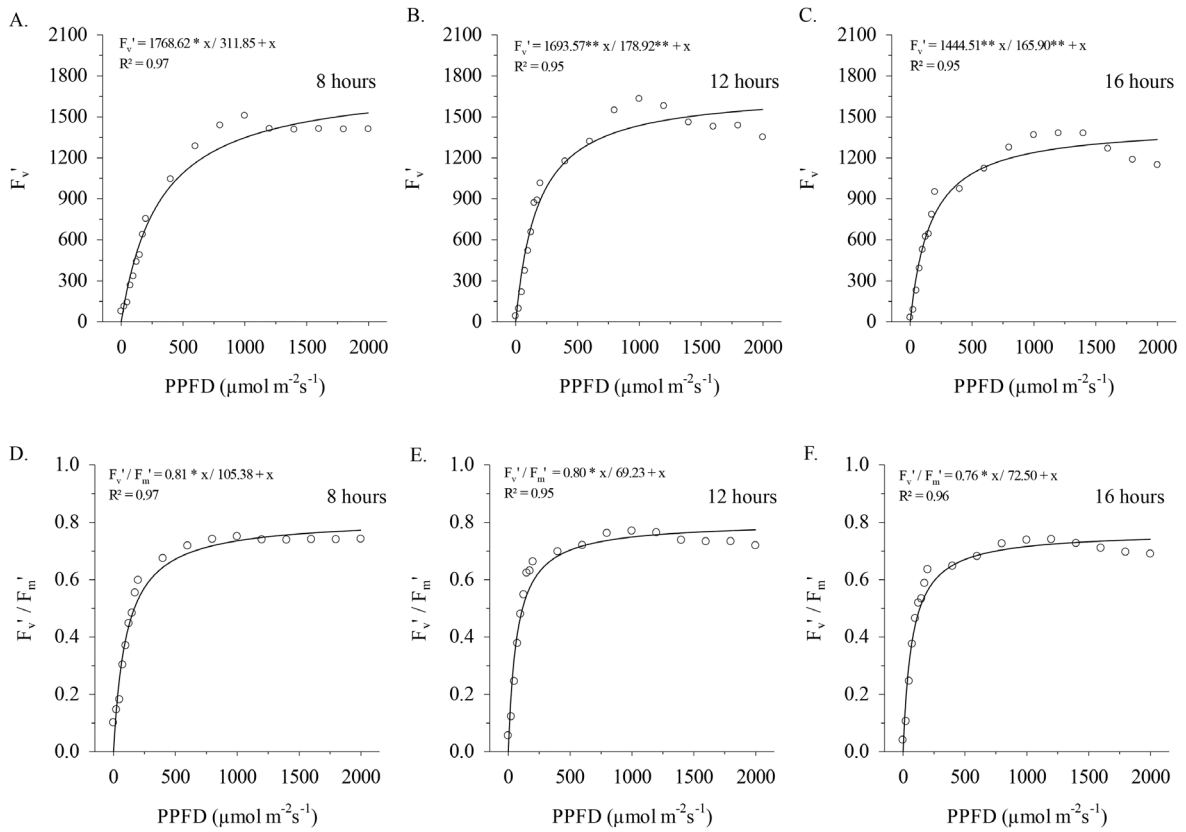
across all evaluation time points in chlorophyll fluorescence parameters between individuals may be due to differences in the concentrations of photoprotective pigments (Takahashi et al., 2011).

The reduction in PSII quantum efficiency (RQP) is related to the low efficiency of light energy absorption required for quinone A activity (Kono et al., 2022). This observed decrease indicates that *P. peruviana* plants were stressed at the lowest photon intensities probably due to the photosynthetic damage under these conditions. Values between 0.75 and 0.85 electron quantum<sup>-1</sup> are indicative of an intact photosynthetic apparatus (Soares et al., 2018).

The  $F_v'/F_0'$  ratio reflected a similar trend as that of the other chlorophyll fluorescence parameters, with the highest values recorded at a PPFD of 1000  $\mu\text{mol m}^{-2} \text{s}^{-1}$  at 8:00 a.m. and 12:00 p.m. (Figures 8A and C). In treatments with lower PPFD, we observed the lowest values for the  $F_v'/F_0'$  ratio at all evaluation time points (Figure 8).

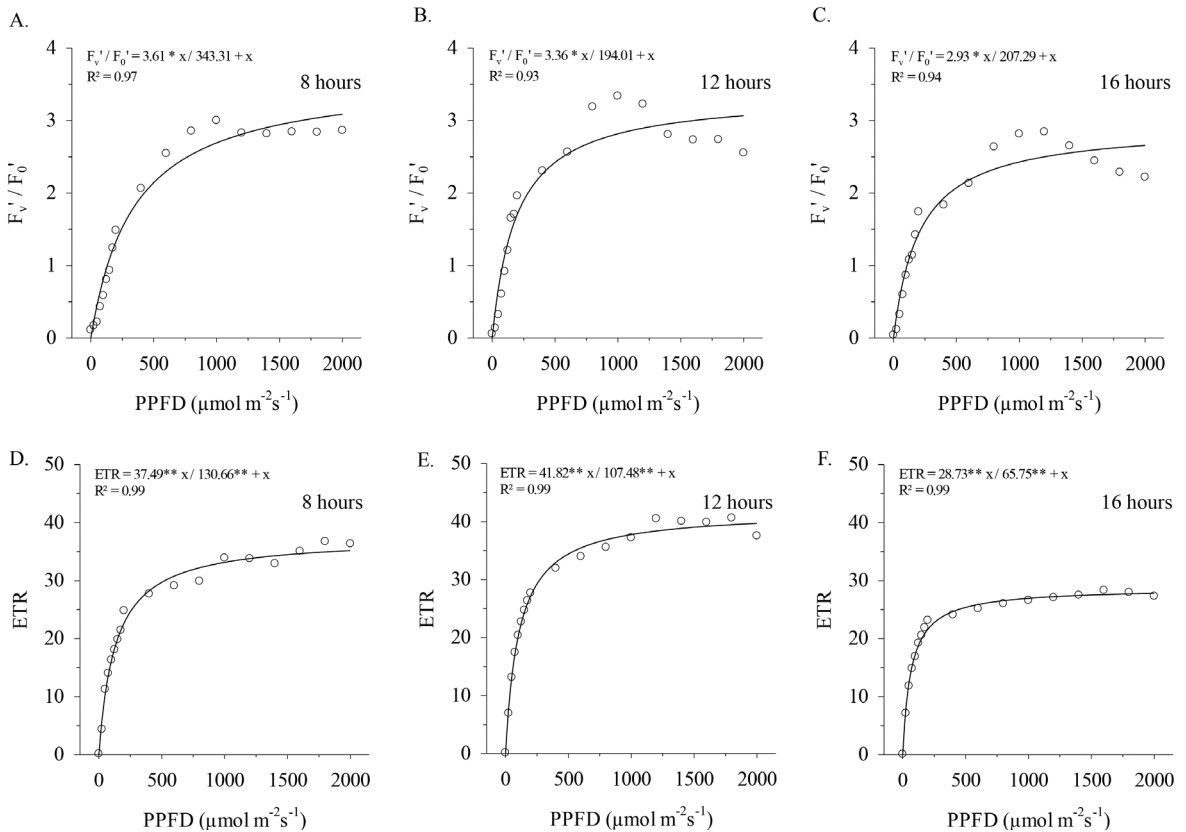
The  $F_v'/F_0'$  ratio is an essential variable that indicates the occurrence of stress because it relates to the flow of absorbed energy and dissipated energy. Therefore, the results observed at a PPFD of 1000  $\mu\text{mol m}^{-2} \text{s}^{-1}$  and 12:00 p.m. indicate that under these conditions, *P. peruviana* plants gain a capacity for efficient energy transfer through PSII (Rai & Agrawal, 2017).

The observed increase in electron transport rate (ETR) can be attributed to photosynthetic acclimation under high PPFD



\*\* - Significant at  $p \leq 0.01$  by F test; \* - Significant at  $p \leq 0.05$  by F test; <sup>ns</sup> - No significant by F test

**Figure 7.** Variable fluorescence ( $F_v'$ ) [(A) 8:00 a.m.; (B) 12:00 p.m.; (C) 4:00 p.m.] and quantum efficiency of the PSII antenna ( $F_v'/F_m'$ ) [(D) 8:00 a.m.; (E) 12:00 p.m.; (F) 4:00 p.m.] in *P. peruviana* plants as a function of photosynthetic photon flux density (PPFD) at different times of day



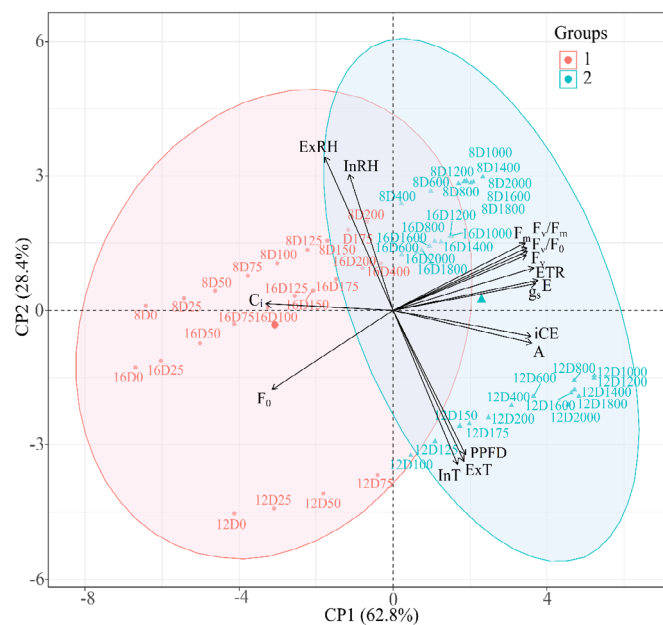
\*\* - Significant at  $p \leq 0.01$  by F test; \* - Significant at  $p \leq 0.05$  by F test; <sup>ns</sup> - No significant by F test

**Figure 8.** Ratio between variable and initial fluorescence ( $F_v'/F_0'$ ) [(A) 8 hours; (B) 12 hours ; (C) 16 hours ] and electron transport rate (ETR) [(D) 8 hours ; (E) 12 hours ; (F) 16 hours] in *P. peruviana* plants as a function of photosynthetic photon flux density (PPFD) at different times of day

conditions (Meng & Runkle, 2019). These results confirm the theory proposed by Bailey et al. (2001) that a high PPFD increases the activity of RuBisCO, the electron transport complex, and ATP synthase. Detection of high electron transport rates during high temperature and irradiance may indicate a greater utilization of resources at the photochemical step, resulting in high photosynthetic rates (Smith & Keenan, 2020).

Principal component analysis (PCA) showed that the dimensions of axes 1 and 2 accounted for 62.8 and 28.4% of the inertia, respectively, corresponding to 91.2% of the total variability of the components (Figure 9). The internal (InT) and external (ExT) air temperature and PPFD showed positive correlations with the net CO<sub>2</sub> assimilation rate (A), instantaneous carboxylation efficiency (iCE), stomatal conductance (g<sub>s</sub>), transpiration (E), electron transport rate (ETR), variable fluorescence (F<sub>v</sub>'), F<sub>v</sub>'/F<sub>0</sub>' ratio, F<sub>v</sub>'/F<sub>m</sub>' ratio, and maximum fluorescence (F<sub>m</sub>') (Figure 8). We observed that the environmental variables of internal (InT) and external (ExT) environmental air temperature and PPFD positively correlated at 12:00 p.m., indicating the influence of these factors on the parameters evaluated at this time point (Figure 9). The eigenvectors of the internal relative and external relative humidity are arranged in the left portion, with negative values indicating a behavior distinct from that of the other variables (Figure 9). Furthermore, a negative correlation was observed between these environmental variables (InRH and ExRH) and Ci and F<sub>0</sub>' (Figure 9).

PPFD had strong positive correlations with all ecophysiological variables, except with Ci and initial



A – net CO<sub>2</sub> assimilation rate; C<sub>i</sub> – Internal CO<sub>2</sub> concentration; g<sub>s</sub> – Stomatal conductance; E – Transpiration; iCE – Instantaneous carboxylation efficiency; F<sub>0</sub>' – Initial fluorescence; F<sub>m</sub>' – Maximum fluorescence; F<sub>v</sub>' – Variable fluorescence; F<sub>v</sub>'/F<sub>0</sub>' – Quantum efficiency of the PSII antenna; F<sub>v</sub>'/F<sub>m</sub>' – Ratio between variable and initial fluorescence; ETR – Electron transport rate; PPFD – Photosynthetic photon flux density; InT – Internal air temperature; ExT – External air temperature; InRH – Internal relative humidity; ExRH – External relative humidity. The numbers before the letter "D" correspond to the evaluation times. The numbers after the letter "D" correspond to photosynthetically active flux densities

**Figure 9.** Principal component analysis between physiological and climatic variables in *P. peruviana* plants for each photosynthetically photon flux density (PPFD) and different times of day

fluorescence, with which it was strongly negatively correlated (Figure 10). Internal (InT) and external (ExT) temperatures were strongly correlated with the net CO<sub>2</sub> assimilation rate (A) and moderately correlated with instantaneous carboxylation efficiency (iCE) and stomatal conductance (g<sub>s</sub>) (Figure 10). Indoor (InRH) and outdoor (ExRH) relative humidity had moderate negative correlations with net CO<sub>2</sub> assimilation and instantaneous carboxylation efficiency (Figure 10).

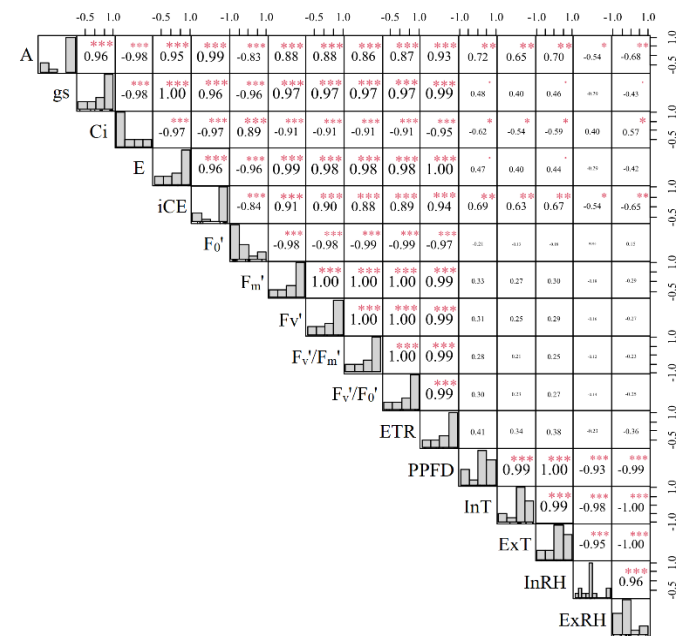


**Figure 10.** Pearson correlation between ecophysiological and climatic variables in *P. peruviana* plants

## CONCLUSIONS

1. Gas exchange and chlorophyll a fluorescence were altered in *P. peruviana* due to photosynthetically active photon flux density (PPFD) and environmental conditions.
2. The higher PPFD (1,384.6  $\mu\text{mol m}^{-2} \text{s}^{-1}$ ) and temperature at 12:00 p.m. favored gas exchange in *P. peruviana*.
3. An increase in PPFD of up to 1000  $\mu\text{mol m}^{-2} \text{s}^{-1}$  increased the chlorophyll a fluorescence in *P. peruviana*.

## LITERATURE CITED

- Alvares, C. A.; Stape, J. L.; Sentelhas, P. C.; Gonçalves, J. L. de M.; Sparovek, G. Köppen's climate classification map for Brazil. Meteorologische Zeitschrift, v.22, p.711-728, 2013. <https://doi.org/10.1127/0941-2948/2013/0507>
- Bailey, S.; Walters, R. G.; Jansson, S.; Horton, P. Acclimation of *Arabidopsis thaliana* to the light environment: the existence of separate low light and high light responses. Planta, v.213, p.794-801, 2001. <https://doi.org/10.1007/s004250100556>
- Baptistella, C. S. L.; Coelho, P. J. Jaboticaba do quintal para produção de mercado. Análises e Indicadores do Agronegócio, v.14, p.1-10, 2019.
- Barbosa, E. A. A.; Digner, E.; Teixeira, W. Z.; Otto, R. F.; Ohse, S. Potencial de água no solo e fertirrigação nitrogenada na produção e trocas gasosas da alface. Revista Brasileira de Agricultura Irrigada, v.13, p.3444-3453, 2019. <https://doi.org/10.7127/rbai.v13n301057>

- Cordeiro, I. M.; Schwartz, G.; Barros, P. L. Efeitos do clima sobre o incremento diamétrico de Paricá (*Schizolobium parahyba* var. Amazonicum-Fabaceae) em plantios comerciais. *Nativa*, v.8, p.246-252, 2020. <https://doi.org/10.31413/nativa.v8i2.9009>
- De Kauwe, M. G.; Medlyn, B. E.; Pitman, A. J.; Drake, J. E.; Ukkola, A.; Griebel, A.; Pendall, E.; Prober, S.; Roderick, M. Examining the evidence for decoupling between photosynthesis and transpiration during heat extremes. *Biogeosciences*, v.16, p.903-916, 2019. <https://doi.org/10.5194/bg-16-903-2019>
- EMBRAPA – Empresa Brasileira de Pesquisa Agropecuária. Manual de métodos de análise de solos. 3.ed. Brasília: Embrapa, 2017. 575p.
- EMBRAPA – Empresa Brasileira de Pesquisa Agropecuária. Sistema Brasileiro de Classificação de Solos. 5.ed. Rio de Janeiro: Embrapa, 2018. 356p.
- Fauset, S.; Oliveira, L.; Buckeridge, M. S.; Foyer, C. H.; Galbraith, D.; Tiwari, R.; Gloor, M. Contrasting responses of stomatal conductance and photosynthetic capacity to warming and elevated CO<sub>2</sub> in the tropical tree species *Alchornea glandulosa* under heatwave conditions. *Environmental and Experimental Botany*, v.158, p.28-39, 2019. <https://doi.org/10.1016/j.envexbot.2018.10.030>
- Griebel, A.; Bennett, L. T.; Metzen, D.; Pendall, E.; Lane, P. N. J.; Arndt, S. K. Trading water for carbon: Maintaining photosynthesis at the cost of increased water loss during high temperatures in a temperate forest. *Journal of Geophysical Research: Biogeosciences*, v.125, p.1-38, 2020. <https://doi.org/10.1029/2019JG005239>
- IBGE - Instituto Brasileiro de Geografia e Estatística. Quantidade produzida, valor da produção, área plantada e área colhida da lavoura temporária: jaboticaba. 2017. Available on: <http://www.sidra.ibge.gov.br>. Accessed on: Nov. 2022.
- Kono, M.; Miyata, K.; Matsuzawa, S.; Noguchi, T.; Oguchi, R.; Suzuki, Y.; Terashima, I. Mixed population hypothesis of the active and inactive PSII complexes opens a new door for photoinhibition and fluorescence studies: an ecophysiological perspective. *Functional Plant Biology*, v.49, p.917-925, 2022. <https://doi.org/10.1071/fp21355>
- Larsen, D. H.; Woltering, E. J.; Nicole, C. C. S.; Marcelis, L. F. M. Response of basil growth and morphology to light intensity and spectrum in a vertical farm. *Frontiers in Plant Science*, v.11, p.1-16, 2020. <https://doi.org/10.3389/fpls.2020.597906>
- Liu, Z. B.; Cheng, R. M.; Xiao, W. F.; Guo, Q. S.; Wang, N. Effect of off-Season flooding on growth, photosynthesis, carbohydrate partitioning, and nutrient uptake in *Distylium chinense*. *Plos One*, v.9, p.1-9, 2014. <https://doi.org/10.1371/journal.pone.0107636>
- Meng, Q.; Runkle, E. S. Far-red radiation interacts with relative and absolute blue and red photon flux densities to regulate growth, morphology, and pigmentation of lettuce and basil seedlings. *Scientia Horticulturae*, v.255, p.269-280, 2019. <https://doi.org/10.1016/j.scienta.2019.05.030>
- Miller, T. E.; Beneyton, T.; Schwander, T.; Diehl, C.; Girault, M.; McLean, R.; Hotel, T.; Noel, P.; Cortina N. S.; Baret, J. C.; Erb, T. J. Light-powered CO<sub>2</sub> fixation in a chloroplast mimic with natural and synthetic parts. *Science*, v.368, p.649-654, 2020. <https://doi.org/10.1126/science.aaz6802>
- Poorter, H.; Niinemets, Ü.; Ntagkas, N.; Siebenkäs, A.; Mäenpää, M.; Matsubara, S.; Pons, T. A meta-analysis of plant responses to light intensity for 70 traits ranging from molecules to whole plant performance. *New Phytologist*, v.223, p.1073-1105, 2019. <https://doi.org/10.1111/nph.15754>
- Rai, K.; Agrawal, S. B. Effects of UV-B radiation on morphological, physiological and biochemical aspects of plants: an overview. *Journal of Scientific Research*, v.61, p.87-113, 2017.
- R Core Team. R: A language and environment for statistical computing. Vienna: R Foundation for Statistical Computing, 2022.
- Ribeiro, J. E. da S.; Barbosa, A. J. S.; Lopes, S. de F.; Pereira, W. E.; Albuquerque, M. B. de. Seasonal variation in gas exchange by plants of *Erythroxylum simonis* Plowman. *Acta Botanica Brasílica*, v.32, p.287-296, 2018. <https://doi.org/10.1590/0102-33062017abb0240>
- Ribeiro, J. E. da S.; Coêlho, E. dos S. Factores abióticos sobre aspectos ecofisiológicos de *Handroanthus impetiginosus* y *Handroanthus serratifolius*. *Bosque*, v.42, p.121-129, 2021. <https://doi.org/10.4067/S0717-92002021000100121>
- Ribeiro, J. E. da S.; Coêlho, E. dos S.; Souza, J. T. A.; Melo, M. F.; Dias, T. J. Climatic variation on gas exchange and chlorophyll a fluorescence in *Tabebuia roseoalba* and *Handroanthus heptaphyllus* (Bignoniaceae). *Brazilian Archives of Biology and Technology*, v.65, p.1-14, 2022. <https://doi.org/10.1590/1678-4324-2022210338>
- Saijo, Y.; Loo, E. P. I. Plant immunity in signal integration between biotic and abiotic stress responses. *New Phytologist*, v.225, p.87-104, 2020. <https://doi.org/10.1111/nph.15989>
- Sharma, A.; Kumar, V.; Shahzad, B.; Ramakrishnan, M.; Sidhu, G. P. S.; Bali, A. S.; Handa, N.; Kapoor, D.; Yadav, P.; Khanna, K.; Bakshi, P.; Rehman, A.; Kohli, S. K.; Khan, E. A.; Parihar, R. D.; Yuan, H.; Thukral, A. K.; Bhardwaj, R.; Zheng, B. Photosynthetic response of plants under different abiotic stresses: a review. *Journal of Plant Growth Regulation*, v.39, p.509-531, 2020. <https://doi.org/10.1007/s00344-019-10018-x>
- Smith, N. G.; Keenan, T. F. Mechanisms underlying leaf photosynthetic acclimation to warming and elevated CO<sub>2</sub> as inferred from least-cost optimality theory. *Global Change Biology*, v.26, p.5202-5216, 2020. <https://doi.org/10.1111/gcb.15212>
- Soares, L. A. dos A.; Fernandes, P. D.; Lima, G. S. de; Brito, M. E. B.; Nascimento, R. do; Arriel, N. H. Physiology and production of naturally-colored cotton under irrigation strategies using salinized water. *Pesquisa Agropecuária Brasileira*, v.53, p.746-755, 2018. <https://doi.org/10.1590/S0100-204X2018000600011>
- Souza, J. T. A.; Ribeiro, J. E. da S.; Ramos, J. P. de F.; Sousa, W. H. de; Araújo, J. S.; Lima, G. F. C.; Dias, J. A. Rendimento quântico e eficiência de uso da água de genótipos de palma forrageira no Semiárido brasileiro. *Archivos de Zootecnia*, v.54, p.283-288, 2019.
- Takahashi, S.; Badger, M. R. Photoprotection in plants: a new light on photosystem II damage. *Trends in plant science*, v.16, p.53-60, 2011. <https://doi.org/10.1016/j.tplants.2010.10.001>
- United States. Soil Survey Staff. Keys to Soil Taxonomy (12.ed.) USDA NRCS. 2014. Available on: <<http://www.nrcs.usda.gov/wps/portal/nrcs/main/soils/survey/>>. Accessed on: Oct. 2022.
- Zhang, Y.; Wang, X.; Pan, Y.; Hu, R.; Chen, N. Global quantitative synthesis of effects of biotic and abiotic factors on stemflow production in woody ecosystems. *Global Ecology and Biogeography*, v.30, p.1713-1723, 2021. <https://doi.org/10.1111/geb.13322>